

Thermal properties and applications of low molecular weight polyhydroxybutyrate

Shinn-Gwo Hong · Heng-Wei Hsu ·
Min-Tzung Ye

Received: 22 December 2011 / Accepted: 18 May 2012 / Published online: 3 July 2012
© Akadémiai Kiadó, Budapest, Hungary 2012

Abstract The properties of the low molecular weight polyhydroxybutyrate (LMWPHB) and LMWPHB plasticized polyhydroxybutyrate (PHB) are studied using differential scanning calorimetry (DSC), thermogravimetric analysis, wide-angle X-ray diffraction (WAXD), polarized optical microscope (POM), mechanical, and biodegradation tests. The results of DSC, WAXD, and POM indicate that LMWPHB has a lower glass transition temperature (T_g), crystallinity, crystallization rate, melting temperature (T_m), and crystal size than PHB due to its much smaller molecular weight. The tensile strength, T_g , T_m , crystallinity, crystallization rate, and thermal stability of LMWPHB plasticized PHB decrease, while the flexibility and biodegradation rate increase with the increasing content of the added LMWPHB. It is confirmed that LMWPHB can be used to improve the brittleness and control the biodegradation rate of PHB.

Keywords Low molecular weight polyhydroxybutyrate · Polyhydroxybutyrate · Biodegradation · Crystallization · Tensile property · Plasticization

Introduction

The biosynthesized polyhydroxyalkanoates (PHAs) have attracted growing attention because of the increasing concerns of the oil shortage and the pursuing of sustainable environments. Among all studied PHAs, the polyhydroxybutyrate (PHB) is of great potential because of its

lowest production cost among PHAs which resulted from its relatively easily biosynthesizable nature [1–7]. However, PHB has inherent inferior properties, e.g., early thermal degradation and brittleness, which seriously limit its acceptance in industry.

The one major drawback of PHB is due to the early degradation happening near its melting temperature. A short exposure of PHB to temperature near 180 °C could induce a severe degradation accompanied by production of the degraded products of olefinic and carboxylic acid compounds, e.g., crotonic acid and various oligomers: through the random chain scission reaction that involves a *cis*-elimination reaction of β -CH and a six-member ring transition [7–9]. The other disadvantage of the brittleness of PHB is attributed to its high degree of crystallization and the post crystallization experienced during the storage, which result in the formation of irregular pores on the surface and limit the flexibility of amorphous chains between the crystals. The results of molecular mechanics calculations also indicate that the secondary crystallization happening on storage can result in a narrow distribution of highly extended or overstressed chains, and subsequently lead to the brittleness of PHB samples [10]. Nonetheless, both the shortcomings of PHB could be alleviated by various modification methods, e.g., the easiest method of adding compatible plasticizers into PHB.

Many materials can be used as plasticizers to improve the toughness of PHB. It is shown that many chemicals, e.g., citrate ester, low molecular weight polyethylene-glycol (PEG), oxypropylated glycerin (or laprol), glycerol, glycerol triacetate, 4-nonylphenol, 4,4'-dihydroxydiphenylmethane, acetyl tributyl citrate, salicylic ester, acetylsalicylic acid ester, soybean oil, epoxidized soybean oil, dibutyl phthalate, triethyl citrate, dioctyl phthalate, dioctyl sebacate, acetyl tributyl citrate, di-2-ethylhexylphthalate, tri(ethylene

S.-G. Hong (✉) · H.-W. Hsu · M.-T. Ye
Department of Chemical Engineering and Materials Science,
Yuan-Ze University, Chung-Li 320, Taiwan
e-mail: cesghong@saturn.yzu.edu.tw

glycol)-bis(2-ethylhexanoate), triacetine, and fatty alcohols with or without glycerol fatty esters, have been investigated as the plasticizers for PHB: many of them proved to have the capability of decreasing the glass transition temperature, and increasing the flexibility (or elongation) and toughness of PHB [11–24]. Although the degradation temperature of the plasticized PHB is decreased compared to the unplasticized PHB, the thermal stability during molding processes could be enhanced, because of the decrease of the melting temperature that resulted from the decrease of crystallinity and the presence of flexible chains of plasticizers.

In this study, the thermal, mechanical, and biodegradation properties of PHB plasticized by the low molecular weight PHB (LMWPHB), which is intrinsically more biodegradable and biocompatible than the mentioned plasticizers, are shown. The uses of LMWPHB that is prepared by different methods have been proposed to make surfactants, graft or block copolymers, additives, compatibilizers, etc. [25–29]. The preparation of LMWPHB takes advantage of the early degradation of PHB at the high temperature. It is demonstrated that the addition of the prepared LMWPHB decreases the crystallinity, crystallization rate, and melting temperature, but increases the flexibility and biodegradation rate of PHB.

Experimental

Preparation of LMWPHB

PHB used is biosynthesized from *E. coli* with crude glucose as the medium (98 % pure obtained from Nan-Tien company with the weight-average molecular weight (M_w) $\approx 750,000 \text{ g mol}^{-1}$, polydispersive index (PDI) ≈ 1.82 , residual Ca^{2+} ($\approx 700 \text{ ppm}$), and Mg^{2+} ($\approx 90 \text{ ppm}$), hermetically stored in a refrigerator below $0 \text{ }^\circ\text{C}$ and randomly selected from different packages). To prepare LMWPHB, the PHB is mixed with polyethylene glycol 400 (PEG 400 from Fluka Chem.) with a ratio of 1:2, purged with nitrogen gas, sealed, and heated at $165 \text{ }^\circ\text{C}$ for 6 h. The reacted PHB is subsequently rinsed with deionized water three times to remove the PEG, filtered, and then dried to obtain LMWPHB (with $M_w = 1,760 \text{ g mol}^{-1}$, $PDI = 1.47$). The molecular weight distributions of LMWPHB are measured by the gel permeation chromatography. The infrared spectrum of LMWPHB is similar to that of PHB, while the result of the proton NMR spectrum of LMWPHB indicates that LMWPHB has extra trans-form unsaturated ends ($\text{CH}_3\text{CH}=\text{CHCOO}^-$) in addition to the main 3-hydroxybutyrate units ($-\text{COOCH}_2\text{CH}_2-$) [30]. The prepared LMWPHB is added into PHB with different weight ratios (LMWPHB: PHB = 1:3 [referred to as PHB-1/4: the specimen with 1/4 LMWPHB], 1:4 (PHB-1/5), 1:5

(PHB-1/6), 1:6 (PHB-1/7), and 1:7 (PHB-1/8)] using chloroform at $50 \text{ }^\circ\text{C}$. Then, LMWPHB/PHB intact films with a thickness about $30 \text{ }\mu\text{m}$ are obtained by the slow evaporation of the chloroform solvent at the room temperature. The prepared dry films are then annealed at $80 \text{ }^\circ\text{C}$ for an hour and stored in the refrigerator below T_g before analyses, to avoid further crystallization during the storage. The tensile properties of the films are measured with an Instron tester at a strain rate of 1 mm min^{-1} from the average of five specimens.

Differential scanning calorimetry (DSC) analyses

A Perkin-Elmer DSC-7 is used to measure the endotherms and exotherms of different specimens. The DSC curves at the heating rate of $10 \text{ }^\circ\text{C min}^{-1}$ from -40 to $185 \text{ }^\circ\text{C}$ (first scan), isotherm at $185 \text{ }^\circ\text{C}$ for 5 min to erase the thermal history, subsequently cooled to $-40 \text{ }^\circ\text{C}$ at a cooling rate of $10 \text{ }^\circ\text{C min}^{-1}$, and then reheated to $185 \text{ }^\circ\text{C}$ at a heating rate of $10 \text{ }^\circ\text{C min}^{-1}$ (second scan), under the nitrogen atmosphere (with a nitrogen flow rate of 40 mL min^{-1}) are measured. Three samples prepared from hermetic aluminum (Al) pans are tested and averaged. The DSC curves obtained are calibrated by the baseline obtained from the empty Al pans and the indium standard.

TG analyses

Different specimens (casted from the 5 wt% chloroform solution with a thickness about 30 micrometers) are further analyzed with a Perkin-Elmer Thermogravimetric Analyzer Pyris-1. The mass-loss behavior of the specimen is measured with a dynamic heating mode. The sample is heated from the room temperature to about $500 \text{ }^\circ\text{C}$ at a heating rate of $10 \text{ }^\circ\text{C min}^{-1}$ with a nitrogen flow rate of 40 mL min^{-1} . The onset and peak temperatures of derivative mass-loss curves and the mass-loss percentages are obtained from TG curves.

Wide-angle X-ray diffraction (WAXD) and polarized optical microscope analyses

The WAXD patterns of specimens (in powders form) which are cooled from $185 \text{ }^\circ\text{C}$ (after 5 min isotherm at $185 \text{ }^\circ\text{C}$ to erase the thermal history) at a cooling rate of $10 \text{ }^\circ\text{C min}^{-1}$ – $50 \text{ }^\circ\text{C}$, and then isothermally crystallized at $50 \text{ }^\circ\text{C}$ for an hour, are taken using XRD-6000 (Shimadza Co., Japan, k_α) at 40 kV and 30 mA) from 2° to 40° at a scanning speed of 1° min^{-1} . The optical images of these isothermally crystallized specimens are also obtained using a Nikon's polarized optical microscope (POM) equipped with a Mettler FP90 heating stage.

Biodegradation test

The prepared films containing different amounts of LMWPHB (3 cm × 3 cm) are enclosed in meshed plastic bags with mesh sizes of about 0.5 mm to let the films freely contact with the humid potting soil (purchased from Greenorchids Com., Taiwan, containing peat moss, perlite, and coconut fibers) but without the loss of the small fragments of the films after long time exposure. The bags are buried vertically in the soil that is placed in a sealed plastic case with saturated water at 25 °C. The test temperature is changed to 35 °C after 35 days. The buried films are periodically removed, thoroughly cleaned with the distilled water, dried in a vacuum oven, and then weighed.

Results and discussion

Characterization of crystalline LMWPHB

The DSC cooling curve of LMWPHB is shown in Fig. 1. For comparison, the cooling DSC curve obtained from the as-received PHB is also shown. As seen, PHB has a crystallization exotherm with an onset temperature at 106.1 °C, a peak crystallization temperature (T_c) about 95.6 °C, and an enthalpy of 70.6 J g⁻¹ that corresponds to a crystallinity of 48.3 % (see Table 1). The cooling characteristics obtained here and those obtained previously have small variations because of the random sampling from low temperature stored PHB, which are all significantly greater than those from LMWPHB. The LMWPHB exhibits a lower onset temperature at 72.4 °C, a lower T_c at about 61.9 °C, and a smaller enthalpy of 35.8 J g⁻¹ representing a lower crystallinity of 24.5 %. These lower values of LMWPHB are attributed to the much lower molecular weight of LMWPHB (see the “Experimental” section) which leads to much greater entropy change during the

Table 1 DSC curves data of PHB and LMWPHB

Cooling	$T_g/^\circ\text{C}$	Onset/ °C	Endset/ °C	$T_c/^\circ\text{C}$	$\Delta H_c/\text{J g}^{-1}$	$X_c/\%$
PHB	-1.0	106.1	87.1	95.6	-70.6	48.3
LMWPHB	-10.0	72.4	53.4	61.9	-35.8	24.5
2nd Heating		Onset/°C	$T_{m1}/^\circ\text{C}$	$T_{m2}/^\circ\text{C}$	$\Delta H_m/\text{J g}^{-1}$	
PHB		155.8	162.5	170.9	80.0	
LMWPHB		70.2	85.5	103.8	38.4	

Standard deviations of all temperature measurements are smaller than 2 °C

Standard deviations of all ΔH measurements are smaller than 3 J g⁻¹

crystallization, retards the crystallization rate, and then results in large differences of the crystallization temperatures and crystallinities obtained. The change in mobility can be confirmed by the significant decrease of the glass transition temperature (T_g) of LMWPHB as shown in Table 1: LMWPHB and PHB have T_g near -10.0 and -1.0 °C, respectively.

As expected, LMWPHB and PHB have different melting characteristics. It is observed in Fig. 2 that the endotherm of PHB has a doublet with peak melting temperatures (T_m) near 162.5 (T_{m1}) and 170.9 °C (T_{m2}), and a melting enthalpy (ΔH_m) of 80.0 J g⁻¹ higher than that of the cooling exotherm due to the secondary crystallization and recrystallization (shown below), while LMWPHB shows a much broader doublet endotherm with much lower T_m near 85.5 and 103.8 °C, and a expected lower ΔH_m of 38.4 J g⁻¹ (Table 1). The melting doublets obtained are known to be resulting from the melting (1st melting peak)—recrystallization—remelting (2nd melting peak) behavior of PHB. However, the relative intensities of the 1st and 2nd peaks of the two specimens are different which indicates that PHB has better crystals with the higher

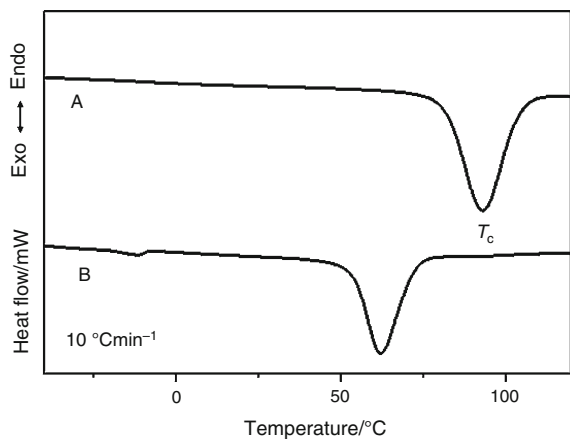


Fig. 1 DSC cooling curves of a PHB and b LMWPHB

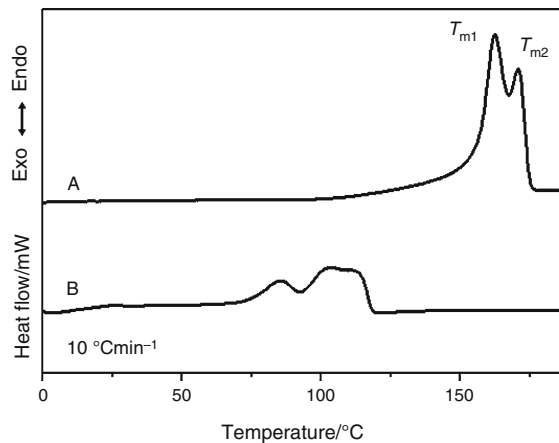


Fig. 2 The 2nd DSC heating curves of a PHB and b LMWPHB

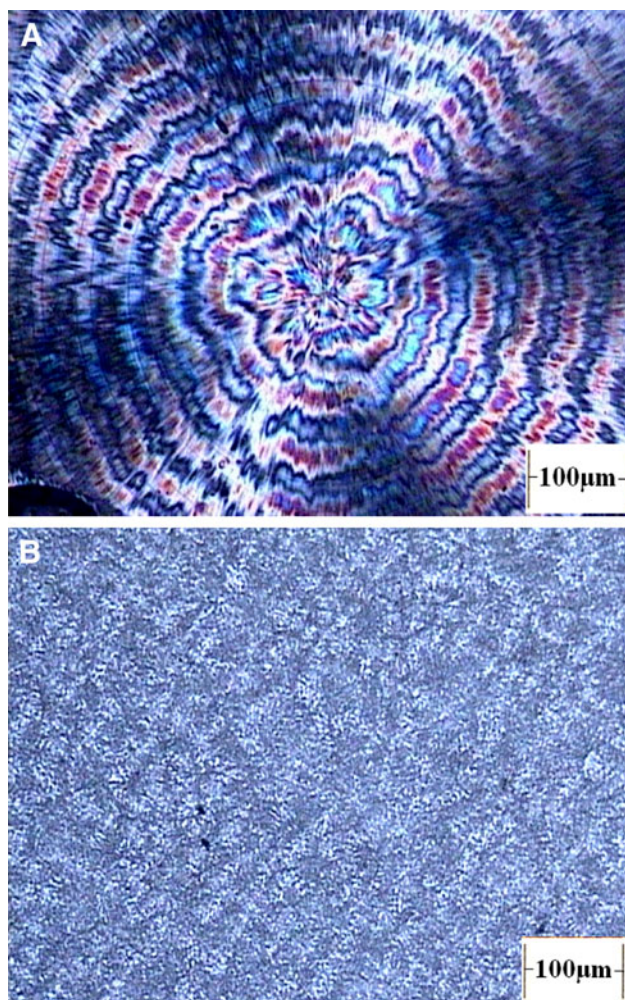


Fig. 3 POM micrographs of **a** PHB and **b** LMWPHB

T_m formed than LMWPHB and then shows a lower extent of recrystallization (1st > 2nd peak) than LMWPHB (1st < 2nd peak). This is confirmed by POM images obtained from the two specimens. In Fig. 3, crystals with a much smaller crystal size and less distinct crystal images are obtained from LMWPHB while crystals with a much greater diameter about 700 μm are seen from PHB. As a result, a much lower T_m but greater degree of the melting—recrystallization—remelting is obtained in LMWPHB.

The crystal structures of PHB and LMWPHB are analyzed by the WAXD of α -form crystals obtained after POM analyses (see Fig. 4). It is obvious that the diffraction patterns and diffraction angles of the two specimens are similar (see Table 2). The lattice parameters calculated by using interplanar distances of planes (020), (110), and (121) in WAXD are shown in Table 2. As obtained, the lattice parameters from LMWPHB are indifferent from those of PHB. The great decreases of the molecular weight of LMWPHB would not affect the basic crystal lattice.

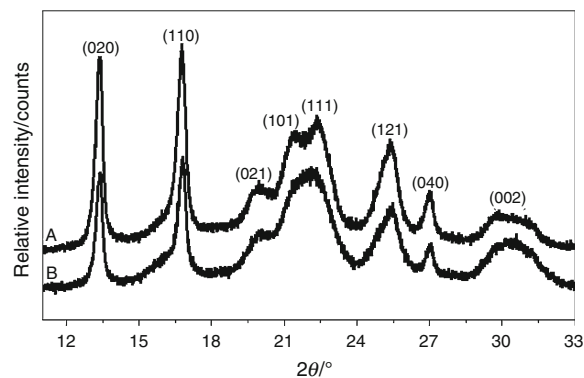


Fig. 4 XRD patterns obtained from **a** PHB and **b** LMWPHB

Properties of LMWPHB modified PHB

The addition of LMWPHB into PHB can change the crystallization behavior of PHB. It is shown in cooling exotherms obtained from PHB samples containing different amounts of LMWPHB that the crystallization exotherms shift to the low temperature side when LMWPHB is added (see Fig. 5). As shown in Table 3, T_c of the samples decreases in the order of PHB > PHB-1/8 > PHB-1/7 > PHB-1/6 > PHB-1/5 > PHB-1/4. The result is attributed to the resulted decreasing concentration of PHB in the samples by adding more mobile but slowly crystallized LMWPHB. The decrease of the crystallization rate can also be confirmed by comparing the differences between the onset and endset temperatures from cooling exotherms which follow the order of PHB (18.9 $^{\circ}\text{C}$) ~ PHB-1/8 (18.4 $^{\circ}\text{C}$) < PHB-1/7 (23.3 $^{\circ}\text{C}$) < PHB-1/6 (27.3 $^{\circ}\text{C}$) < PHB-1/5 (29.8 $^{\circ}\text{C}$) < PHB-1/4 (33.2 $^{\circ}\text{C}$) indicating that the more the LMWPHB is added, the more the time is needed to crystallize.

In addition, the crystallinity of PHB also has changed in the presence of LMWPHB. It is shown in Table 3 that the crystallization enthalpy (ΔH_c), i. e., the crystallinity of PHB decreases with the increasing LMWPHB content and follows the order of PHB > PHB-1/8 ~ PHB-1/7 > PHB-1/6 ~ PHB-1/5 > PHB-1/4. This result is expected because the added compatible LMWPHB has a smaller crystallinity than PHB.

The compatibility of LMWPHB and PHB is doubtless due to the same chemical structure of the main chains. The result of T_g also confirms the good miscibility of LMWPHB in PHB because of only one T_g observed in all samples. It is expected that T_g of LMWPHB/PHB samples decreases with the increasing content of LMWPHB and with the order of PHB (5.3 $^{\circ}\text{C}$) > PHB-1/8 (-2.6 $^{\circ}\text{C}$) > PHB-1/7 (-3.9 $^{\circ}\text{C}$) > PHB-1/6 (-4.8 $^{\circ}\text{C}$) > PHB-1/5 (-6.3 $^{\circ}\text{C}$) > PHB-1/4 (-7.3 $^{\circ}\text{C}$) (obtained from a fast heating rate of 50 $^{\circ}\text{C min}^{-1}$ in order to increase the

Table 2 XRD patterns of PHB and LMWPHB

2 θ /degree	(020)	(110)	(021)	(101)	(111)	(121)	(040)	(002)
PHB	13.34	16.73	19.95	21.43	22.36	25.28	26.96	29.74
LMWPHB	13.35	16.75	19.99	–	22.05	25.27	26.98	29.80
Lattice constants			$a/\text{\AA}$			$b/\text{\AA}$		$c/\text{\AA}$
PHB			5.77			13.27		5.98
LMWPHB			5.76			13.26		6.00

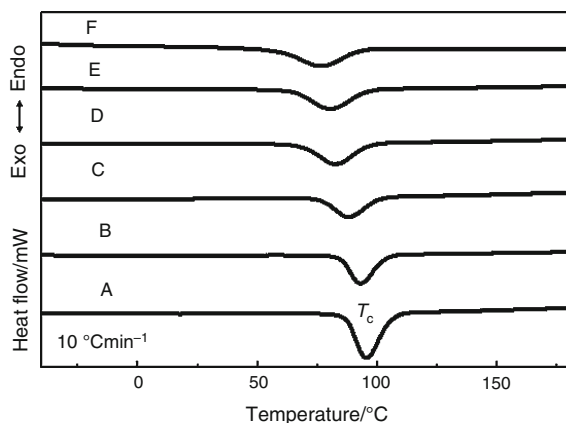
sensitivity of T_g measurements by DSC). The LMWPHB acts like a plasticizer in PHB which increases the mobility but decreases the T_g of PHB.

It is interesting to note that the decrease of ΔH_c in samples does not change linearly with respect to the content of added LMWPHB. For example, the PHB-1/4 has ΔH_c about 55.3 J g^{-1} but it should have ΔH_c near 61.9 J g^{-1} if the linear combination of ΔH_c from PHB ($\Delta H_c = 70.6 \text{ J g}^{-1}$) and LMWPHB ($\Delta H_c = 35.8 \text{ J g}^{-1}$) is followed. This is attributed to the facts that the presence of LMWPHB not only increases the mobility/flexibility of PHB (plasticizing effect) but also correspondingly decreases the real concentration of PHB crystals formed during the cooling process. As the crystallization of PHB is

finished, the crystallization of LMWPHB is also restricted in the solid solution and which is confirmed by the absence of the exothermic peak of LMWPHB (with a T_c near $61.9 \text{ }^\circ\text{C}$) in Fig. 5 (also see Fig. 1).

The change of crystallization behaviors also affects the melting endotherms obtained. It is shown in Fig. 6, the heating endotherms obtained from crystallized samples after cooled in DSC at a rate of $10 \text{ }^\circ\text{C min}^{-1}$, that the melting temperatures and melting peaks of the samples are all different. Despite the fact that all the samples exhibit two melting peaks because of the aforementioned melting-recrystallization-remelting behavior of PHB, the melting temperatures, T_{m1} and T_{m2} , decrease significantly with the increasing amount of LMWPHB and in the order of PHB > PHB-1/8 ~ PHB-1/7 > PHB-1/6 ~ PHB-1/5 > PHB-1/4 (see Table 4). The difference between T_{m1} and T_{m2} in the samples also noticeably increases with the LMWPHB content. This result confirms that the plasticizing effect of LMWPHB results in the formation of not well crystallized PHB with a wider distribution of crystal sizes that melt at the lower but broader melting temperatures.

The formation of crystals with a low T_m can also be confirmed by comparing the relative intensities of doublet peaks in endotherms. As shown in Fig. 6, the 1st melting peak decreases, while 2nd melting peak increases in

**Fig. 5** DSC cooling curves of a PHB, b PHB-1/8, c PHB-1/7, d PHB-1/6, e PHB-1/5, and f PHB-1/4**Table 3** DSC cooling curves data of LMWPHB modified PHB

Specimens	$T_c/^\circ\text{C}$	$\Delta H_c/\text{J g}^{-1}$	$X_c/\%$
PHB	95.6 ± 2	$-70.6 \pm 2^*$	48.3
PHB-1/8	93.2 ± 2	-65.5 ± 4	44.8
PHB-1/7	88.3 ± 2	-64.3 ± 2	44.0
PHB-1/6	82.1 ± 2	-59.1 ± 1	40.4
PHB-1/5	80.3 ± 1	-58.8 ± 3	40.2
PHB-1/4	76.7 ± 1	-55.3 ± 2	37.8

* \pm Standard deviation

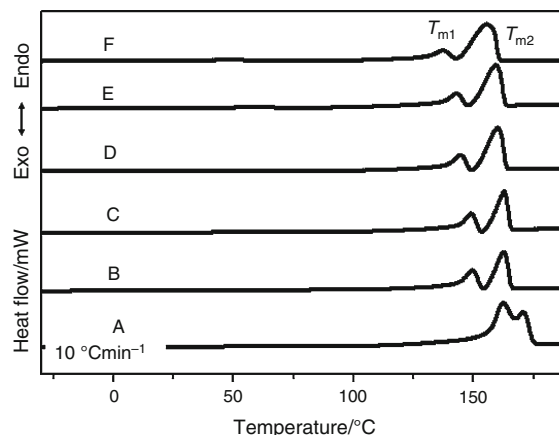
**Fig. 6** DSC 2nd heating curves of a PHB, b PHB-1/8, c PHB-1/7, d PHB-1/6, e PHB-1/5, and f PHB-1/4

Table 4 DSC 2nd heating curves data of LMWPHB modified PHB

Specimens	Onset/°C	$T_{m1}/^{\circ}\text{C}$	$T_{m2}/^{\circ}\text{C}$	$\Delta H_m/\text{J g}^{-1}$
PHB	155.2 ± 2*	162.5 ± 3	170.9 ± 1	80.0
PHB-1/8	110.4 ± 2	149.2 ± 2	162.3 ± 1	71.4
PHB-1/7	111.3 ± 3	148.1 ± 1	162.2 ± 1	68.7
PHB-1/6	111.4 ± 2	144.7 ± 4	160.5 ± 3	68.5
PHB-1/5	111.3 ± 3	143.6 ± 4	159.5 ± 2	65.2
PHB-1/4	109.5 ± 4	137.3 ± 1	155.8 ± 1	64.2

Standard deviations of all ΔH_m measurements are smaller than 3 J g⁻¹

* ±Standard deviation

intensities with increasing LMWPHB content in samples. As the 1st lower T_{m1} peak is mostly resulted from the melting of crystals formed during the cooling crystallization and the 2nd higher T_{m2} peak is related to the recrystallization—remelting after the 1st melting, the result indicates that the more the LMWPHB is added in PHB, the more the less-perfect or smaller crystals melting at a lower temperature would be formed and which leads to more crystals formed through the recrystallization process. As a result, a larger 2nd melting peak is obtained from the specimen with a greater LMWPHB content.

As expected from ΔH_c , ΔH_m obtained also decreases with the increasing LMWPHB content and with the order of PHB > PHB-1/8 > PHB-1/7 ~ PHB-1/6 > PHB-1/5 ~ PHB-1/4 (see Table 4). However, it is noticed that ΔH_m obtained after normalized by the content of PHB are 80.0 J g⁻¹ for PHB, 81.6 J g⁻¹ for PHB-1/8, 80.1 J g⁻¹ for PHB-1/7, 82.2 J g⁻¹ for PHB-1/6, 81.5 J g⁻¹ for PHB-1/5, and 85.6 J g⁻¹ for PHB-1/4 which show few differences except that of PHB-1/4. The result is consistent with those obtained from T_c , T_m , and ΔH_c that LMWPHB has negligible crystallization in PHB. Nonetheless, some LMWPHB in the samples may also crystallize through the

2nd crystallization during the heating step if abundant amounts of LMWPHB are added, e.g., PHB-1/4.

The thermal stability of PHB is adversely affected by the presence of LMWPHB. The representative TG curves obtained from PHB, PHB-1/6, and PHB-1/4 are shown in Fig. 7. The onset degradation temperatures of the samples follows the order of PHB (228.8 °C) > PHB-1/6 (218.2 °C) > PHB-1/4 (210.6 °C) (all with a standard deviation less than 3.0 °C). It is also obtained that PHB has a peak degradation temperature (248.6 °C) higher than PHB-1/6 (240.1 °C) and PHB-1/4 (235.7 °C). As a result, LMWPHB decreases the thermal stability of the samples because its small molecular weight causes it to degrade at a low temperature. The more LMWPHB is added, the worse is the thermal stability obtained.

The plasticizing effect of LMWPHB on the tensile properties of various LMWPHB/PHB samples is also tested. From the representative tensile stress–strain curves shown in Fig. 8, it is clear that the ultimate tensile strength (σ_T) and elongation at break (ϵ) of the samples vary with the content of LMWPHB. PHB, PHB-1/8, PHB-1/7, and PHB-1/6 have similar nominal σ_T as standard deviations are considered (see Table 5). However, the elongation

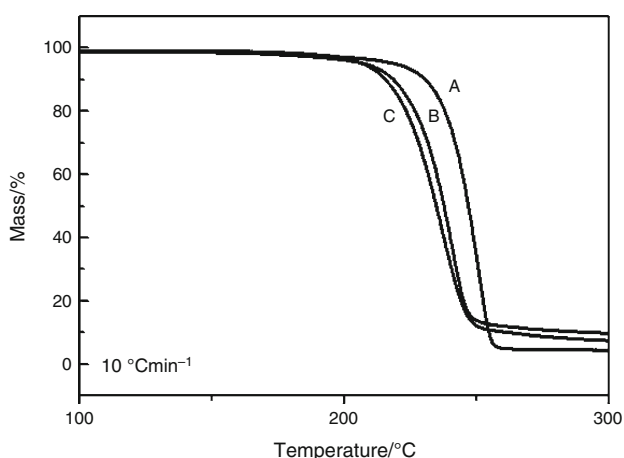
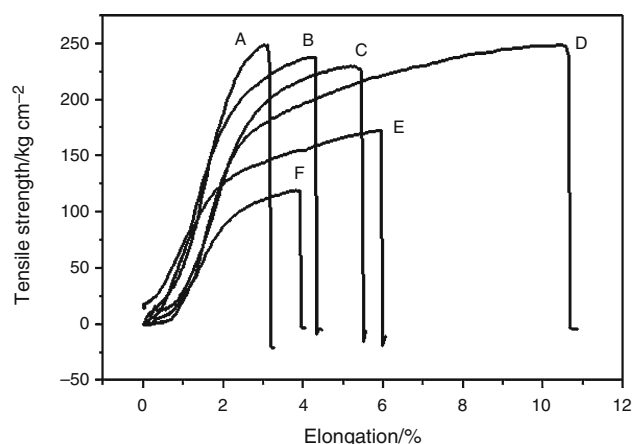
**Fig. 7** TG curves obtained from a PHB, b PHB-1/6, and c PHB-1/4**Fig. 8** The stress–strain relations obtained from a PHB, b PHB-1/8, c PHB-1/7, d PHB-1/6, e PHB-1/5, and f PHB-1/4

Table 5 Tensile properties of LMWPHB modified PHB

Specimens	Elongation at break/%	Tensile strength/kg cm ⁻²
PHB	3.1 ± 0.3*	248 ± 10
PHB-1/8	4.2 ± 0.2	237 ± 10
PHB-1/7	5.6 ± 0.6	229 ± 15
PHB-1/6	9.8 ± 1.0	248 ± 17
PHB-1/5	6.1 ± 0.3	172 ± 15
PHB-1/4	3.8 ± 0.3	119 ± 17

* ±Standard deviation

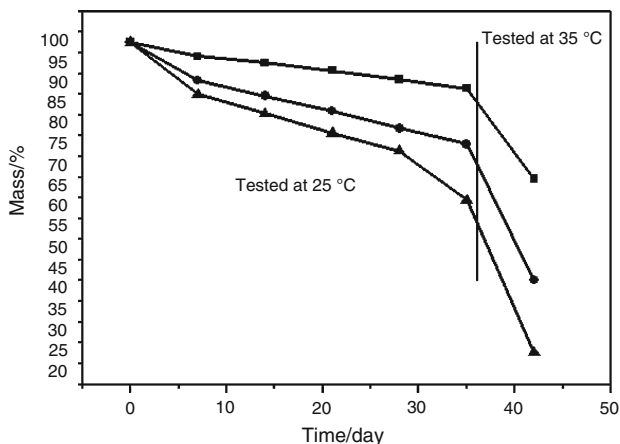
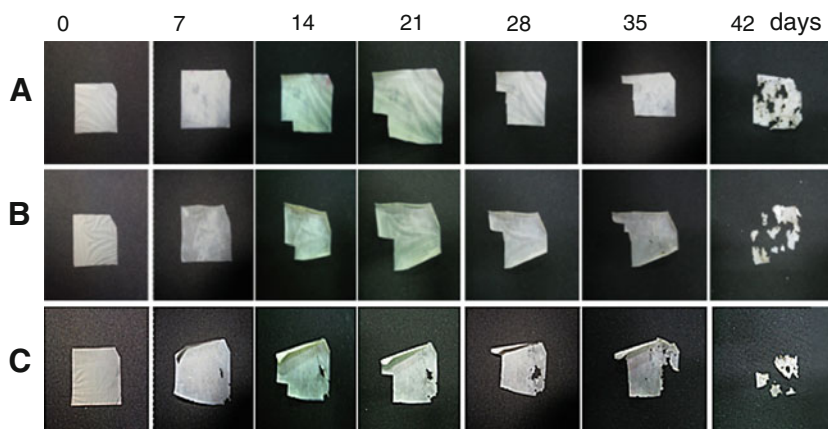


Fig. 9 The mass changes of (a) PHB squares, (b) PHB-1/6 circles, and (c) PHB-1/4 triangles during the biodegradation test

could be greatly changed by the added LMWPHB. As observed in Fig. 8 and Table 5, the ϵ of the samples increases with the increasing LMWPHB content and follows the order of PHB < PHB-1/8 < PHB-1/7 < PHB-1/6. The plasticizing effect of LMWPHB on improving the flexibility of PHB is confirmed, and the best tensile performance is obtained from PHB with 1/6 LMWPHB. The improvement is significant since the brittle PHB usually has a much low ϵ below 3%. In addition, the actual σ_T of PHB-1/6 is much higher than its nominal σ_T because the strain-induced crystallization causes appreciable increase

Fig. 10 The changes of film integrity from samples a PHB, b PHB-1/6, and c PHB-1/4 during the biodegradation test



of ϵ , which is confirmed by the characteristic long, flat stress–strain curve of PHB-1/6.

Nonetheless, an excess amount of LMWPHB added could degrade tensile properties of PHB. It is shown in Table 5 that PHB-1/5 and PHB-1/4 have nominal σ_T near 172 and 119 kg cm⁻², respectively, which are significantly lower than those of other specimens (also see Fig. 8). Not only σ_T , but also ϵ of the both samples are obviously lower than that of PHB-1/6. The observed changes are attributed to the small strength of LMWPHB which decreases the strength of PHB notably as the failure is initiated in the abundant LMWPHB. As a result, the more than enough LMWPHB is added, and the lower σ_T or ϵ is obtained.

The presence of LMWPHB would accelerate the biodegradation rate of PHB. The mass-losses of representative samples during the biodegradation test are shown in Fig. 9. As observed, the biodegradation rates of the samples significantly increase with the increasing LMWPHB content. The unadded PHB lost about 10.5% mass after 5 weeks in the humid potting soil at the room temperature, while PHB-1/6 and PHB-1/4 lost much greater mass of 22.2 and 37.8%, respectively, in the same period. It is well known that the amorphous regions of PHB are much more easily attacked by microorganisms than the crystalline regions. As obtained previously, a higher content of LMWPHB in the samples would result in a lower crystallinity of PHB, subsequently, also lead to a faster degradation rate. In addition, the lower T_g and less rigidity of the LMWPHB added PHB can also facilitate the biodegradation process because of the easier penetration of water and micro-organisms.

An increase of the testing temperature can drastically accelerate the biodegradation rate. It is shown in Fig. 9 that all three samples lose a lot of masses, 21.8% from PHB, 32.9% from PHB-1/6, and 36.7% from PHB-1/4, during the 7th week in which the testing temperature is changed from 25 °C to a higher 35 °C. In addition, the samples of PHB-1/6 and PHB-1/4 were also broken into small pieces after such a great mass-loss (see Fig. 10). The film of PHB, with a smaller total mass-loss of 32.3% (10.5 + 21.8%),

basically remained its integrity but with many pores. The results of biodegradation test indicate that the addition of LMWPHB can be used to control the biodegradation rate of PHB, tailor the strength (sample integrity) of PHB products with respect to the exposure conditions, and then lead to a lot of industrial applications.

Conclusions

The properties of the LMWPHB and PHB plasticized with LMWPHB are shown. It is indicated that LMWPHB has a lower glass transition temperature (T_g), crystallinity, crystallization rate, melting temperature (T_m), and crystal size than PHB. The addition of LMWPHB can decrease the tensile strength, T_g , T_m , crystallinity, crystallization rate, and thermal stability, but increase the flexibility and biodegradation rate of PHB. The extent of the changes increases with the increasing amount of LMWPHB added. It is concluded that LMWPHB has a great potential in industrial applications because of its capabilities of improving the brittleness and controlling the biodegradation rate of PHB and other similar materials.

References

- Mas-Castella J, Urmeneta J, Lafuente R, Navarrete A, Guerrero R. Biodegradation of poly- $[\beta]$ -hydroxyalkanoates in anaerobic sediments. *Int Biodeterior Biodegrad*. 1995;35:155–74.
- Doi Y, Kasuya K, Abe H, Koyama N, Ishiwatari S, Takagi K, Yoshida Y. Evaluation of biodegradabilities of biosynthetic and chemosynthetic polyesters in river water. *Polym Degrad Stab*. 1996;51:281–6.
- Yoon JS, Jung HW, Kim MN, Park ES. Diffusion coefficient and equilibrium solubility of water molecules in biodegradable polymers. *J Appl Polym Sci*. 2000;77:1716–22.
- Kumagai Y, Kanesawa Y, Doi Y. Enzymatic degradation of microbial poly(3-hydroxybutyrate) films. *Makromol Chem*. 1992;193: 53–7.
- Iwata T, Shiromo M, Doi Y. Surface structures of poly[(R)-3-hydroxybutyrate] and its copolymer single crystals before and after enzymatic degradation with an extracellular PHB depolymerase. *Macromol Chem Phys*. 2002;203:1309–16.
- Koyama N, Doi Y. Effects of solid-state structures on the enzymatic degradability of bacterial poly(hydroxyalkanoic acids). *Macromolecules*. 1997;30:826–32.
- Doi Y, Mukai K, Kasuya K, Yamada K: Biodegradation of biosynthetic and chemosynthetic polyhydroxyalkanoates. In: Doi Y, Fukuda K, editors. *Biodegradable Plastics and Polymers*. Elsevier, Amsterdam; 1994, p. 39–51.
- Grassie N, Marray EJ, Holmes PA. The thermal degradation of poly(-D)- β -hydroxybutyric acid): part 1—identification and quantitative analysis of products. *Polym Degrad Stab*. 1984;6: 47–61.
- Grassie N, Marray EJ, Holmes PA. The thermal degradation of poly(-D)- β -hydroxybutyric acid): part 2—changes in molecular weight. *Polym Degrad Stab*. 1984;6:95–103.
- Spitalsky Z, Bleha T. Elastic properties of poly(-D)- β -hydroxybutyrate) molecules. *Macromol Biosci*. 2004;4(6):601–9.
- Bibers I, Tupureina V, Dzene A, Savenkova L, Kalnins M. Biodegradable materials from plasticized PHB biomass. *Macromol Symp*. 2001;170:61–72.
- Janigova' I, Lack I, Chodak I. Thermal degradation of plasticized poly(3-hydroxybutyrate) investigated by DSC. *Polym Degrad Stab*. 2002;77:35–41.
- Garcia-Lopera R, Monzo IS, Porcar I, Abad C, Campos A. Miscibility of blends of biodegradable polymers and copolymers with different plasticizers. *Macromol Chem Phys*. 2008;209:2147–56.
- Erceg M, Kovacic T, Klaric I. Thermal degradation of poly(3-hydroxybutyrate) plasticized with acetyl tributyl citrate. *Polym Degrad Stab*. 2005;90:313–8.
- Kunze C, Freier T, Kramer S, Schmitz KP. Anti-inflammatory prodrugs as plasticizers for biodegradable implant materials based on poly(3-hydroxybutyrate). *J Mater Sci*. 2002;13:1051–5.
- Choi JS, Park WH. Effect of biodegradable plasticizers on thermal and mechanical properties of poly(3-hydroxybutyrate). *Polym Test*. 2004;23:455–60.
- Wang L, Zhu W, Wang X, Chen X, Chen GQ, Xu K. Processability modifications of poly(3-hydroxybutyrate) by plasticizing, blending, and stabilizing. *J Appl Polym Sci*. 2008;107:166–73.
- Erkske D, Viskere I, Dzene A, Tupureina V, Savenkova L. Biobased polymer composites for films and coatings. *Proc Estonian Acad Sci Chem*. 2006;55:70–7.
- Dukalska L, Muizniece-Brasava S, Kampuse S, Seglina D, Straumite E, Galoburda R, Levkane V. Studies of biodegradable polymer material suitability for food packaging applications. *Jelgava: FOODBALT*; 2008. p. 64–8.
- Muizniece-Brasava S, Dukalska L. Impact of biodegradable PHB packaging composite materials on dairy product quality. *Proc LUA*. 2006;16(311):81–9.
- Ceccorulli G, Pizzoli M, Scandola M. Effect of a low molecular weight plasticizer on the thermal and viscoelastic properties of miscible blends of bacterial poly(3-hydroxybutyrate) with cellulose acetate butyrate. *Macromolecules*. 1993;26:6722–6.
- Fernandes EG, Pietrini M, Chiellini E. Bio-based polymeric composites comprising wood flour as filler. *Biomacromolecules*. 2004;5:1200–5.
- Vašková I, Alexy P, Bugaj P, Nahálková A, Feranc J, Mlynský T. Biodegradable polymer packaging materials based on polycaprolactone, starch and polyhydroxybutyrate. *Acta Chim Slovaca*. 2008;1(1):301–8.
- Almeida D, Bueno W, Bizzari PS, Durao NAS, Do Nascimento JF. Use of fatty alcohols as plasticizer to improve the physical-mechanical properties and processability of Phb and its copolymers. *United States Patent Pub. No.: US20080139702*, 2008.
- Oh WG, Kim BS. Novel biodegradable molecularly imprinted polymers based on poly(3-hydroxybutyrate). *Macromol Symp*. 2007;249–250:76–80.
- Yu G, Marchessault RH. Characterization of low molecular weight poly(b-hydroxybutyrate)s from alkaline and acid hydrolysis. *Polymer*. 2000;41:1087–98.
- Špitalský Z, Lack I, Lathová E, Janigová I, Chodák I. Controlled degradation of polyhydroxybutyrate via alcoholysis with ethylene glycol or glycerol. *Polym Degrad Stab*. 2006;91:856–61.
- Nguyen S, Yu G, Marchessault RH. Thermal degradation of poly(3-hydroxyalkanoates): preparation of well-defined oligomers. *Biomacromolecules*. 2002;3:219–24.
- Yu G. Process of producing low molecular weight poly(hydroxyalkanoate)s from high molecular weight poly(hydroxyalkanoate)s. *United States Patent Pub. No.: US20050260723*, 2005.
- Hsu HW. Effects of the characteristics and addition of low molecular weight poly-3-hydroxyalkanoate on the physical properties of specific polymers. *Master Thesis, Yuan-Ze University, Taiwan*; 2010, p. 58.